Gamma-ray studies of $^{12}C+^{20}Ne$ reactions

P. A. DeYoung, J. J. Kolata, R. C. Luhn, R. E. Malmin, and S. N. Tripathi
Physics Department, University of Notre Dame, Notre Dame, Indiana 46556
(Received 1 June 1981)

Excitation functions for the yields of ten residual nuclides from the $^{12}C+^{20}Ne$ reaction have been measured over the range $E_{c.m.}=11-33$ MeV in steps of 150 keV, using γ-ray techniques. The magnitude and energy dependence of the excitation functions for most partial yields, as well as for the total fusion yield, closely resemble those from the $^{16}O+^{16}O$ system when compared at the same compound-nuclear excitation energy. The total fusion yield exhibits strong anomalies at $E_{c.m.}=22.7$ and 24.1 MeV, while the ^{20}Ne inelastic scattering yield exhibits a strong uncorrelated structure at $E_{c.m.}=21.1$ MeV. In addition weaker structure is seen at $E_{c.m.}=13.6$, 16.6, 18.6, and 26.3 MeV in the total fusion yield. The 24.1 MeV resonance corresponds to a characteristic structure in the $^{16}O+^{16}O$ reaction yields. Both structures appear at the same ^{32}S excitation energy and are found to be correlated with the transition to a regime of limited fusion.

[NUCLEAR REACTIONS $^{20}Ne(^{12}C,x)$; $E_{c.m.}=11-33$ MeV; measured excitation functions for production of $A=20-30$ reaction products; observed structure at $E_{c.m.}=(13.6)$, 16.6, 18.6, 21.1, 22.7, 24.1, and 26.3 MeV; deduced critical angular momentum for fusion.]

I. INTRODUCTION

The identical particle $^{16}O+^{16}O$ system exhibits resonantlike structure[1-6] in its fusion cross section which was found[1] to be anticorrelated with similar features in the $\theta_{c.m.}=90°$ elastic-scattering excitation function.[7] In addition, it has recently been shown that for $^{16}O+^{16}O$, as well as for several other systems, a sharp break in the trajectory of the critical angular momentum deduced from the fusion cross section occurs where the trajectory intersects the extended ground-state band of the compound nucleus.[8] This abrupt transition to a regime of limited fusion was shown to be associated with a characteristic "resonance" in certain reaction yields which occurs at the crossover point between the low-energy and high-energy behavior of the critical angular momentum. The $^{12}C+^{20}Ne$ reaction provides a nearly ideal case for testing whether any or all of these features are unique to the $^{16}O+^{16}O$ system, or if they are in fact more general. It also provides an opportunity to determine whether the observed phenomena are entrance channel effects or due to some property of the compound nucleus. The two systems are extraordinarily well matched[9] in Q-value and angular momentum, so that at equal center-of-mass (c.m.) energies one is probing similar regions of energy and angular momentum in the compound nucleus and in the optical-model potential. It was anticipated that the asymmetric nature of the entrance channel in the case of $^{12}C+^{20}Ne$ would serve to reduce or eliminate any structure in the fusion yield, since the restriction to only even partial waves as in $^{16}O+^{16}O$ would not apply. This view was supported by the smooth behavior of the elastic scattering excitation function measured by Vandenbosch *et al.*[9] However, prominent structure was observed in the fusion yield and the possible implications of this observation will be discussed. In addition, we will report on several "resonant" anomalies in the measured inelastic scattering and fusion yields, one of which has the properties of the characteristic resonance discussed above. It will be shown that this structure appears at exactly the same excitation energy in ^{32}S in both reactions, thus establishing that these characteristic resonances are a property of the compound system rather than of the entrance channel.

II. EXPERIMENTAL METHOD AND RESULTS

The experiment was performed using a ^{12}C beam from the University of Notre Dame three-stage tandem Van de Graaff accelerator. The range of beam energies used was $E_{lab}=20-53.5$ MeV, and over most of the energy range the step size was 250 keV. The target was typically 25 $\mu g/cm^2$ of ^{20}Ne, isotopically enriched to 99.96%, contained in a gas cell (Fig. 1) consisting of a bored out Pb brick, a thin Ni window (450 $\mu g/cm^2$) to contain the gas at a typical pressure of 30 torr, and a Au-backed thin-walled Al cylinder which comprised the target volume.[10] The gas continuously flowed through the cell to avoid contamination problems, and the pressure was regulated with a Cartesian-diver manostat.

Gamma rays were detected by a 90 cm^3 Ge(Li) detector placed at 55° to the beam and 5 cm from the target. The detector was shielded from γ rays originating from reactions in the window or upstream collimators by the Pb body of the cell and, when needed, by additional Pb shielding. The effectiveness of the shielding was checked by removing the gas from the cell at one point during the experiment. Under these conditions, only Coulomb excitation of the thick Au beam stop was observed. The primary relative normalization of the data, which was derived from these Coulex transitions, agreed to within 1.5% (rms deviation) with that obtained from charge collection of the beam striking the cell, window, and brick (which were connected together electrically and maintained at + 300 V relative to ground). In practice it is only necessary to assume that the Coulex cross section is locally smooth, since charge collection will determine the correct long-term behavior. Nevertheless, the measured Au Coulex yields are in excellent agreement with the predictions of a thick target Winther-deBoer multiple-Coulomb-excitation program,[11] as regards both short and long range behavior. The absolute normalization was determined by comparison with the ^{20}Ne yield from the $^{12}C+^{16}O$ reaction at $E_{c.m.}=19.0$ and 22.9 MeV. The relative normalizations of the two C+O runs were performed as described above. Corrections were made to account for the differences in gas pressure between the ^{20}Ne and ^{16}O runs, the diatomic nature of the O_2 gas used, and the efficiency function of the Ge(Li) detector. The estimated uncertainty in the normalization is 11%, primarily due to the 7% uncertainty in the absolute normalization[12] of the $^{12}C+^{16}O$ reaction yields.

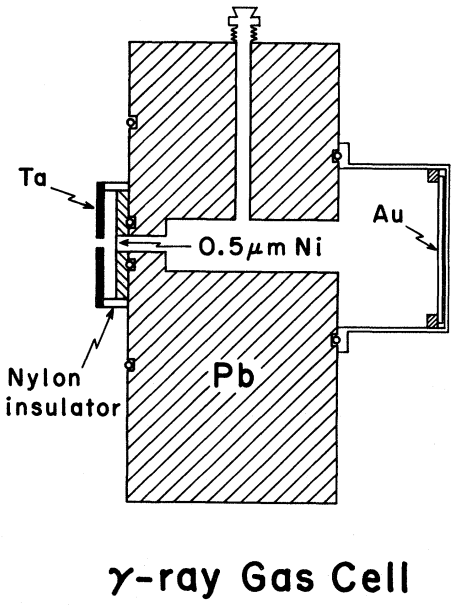

FIG. 1. A cross sectional view of the gas cell used for this work. The detector was located in a plane perpendicular to the page and containing the beam and placed at an angle of 55° to the beam.

A spectrum from the $^{12}C+^{20}Ne$ reaction is shown in Fig. 2 while Table I lists those γ-ray transitions which were used to determine the yields of various residual nuclei. In all cases only the shifted components of a particular line shape have been used in determining a particular yield to insure that there is no contribution from reactions within the body of the gas cell. However, for those γ-rays resulting from the decay of long lived levels, this treatment may result in incorrect yields. If the reaction products are formed outside the region of the aluminum cell they may travel into the aluminum cell before decaying, resulting in increased measured yields. Alternately, some reaction products formed in the cell may be stopped in the Au backing before decaying, appearing as narrow lines resulting in decreased measured yields. In the $^{12}C+^{20}Ne$ system this situation arises with the 417 keV line from ^{26}Al. However, given the particular velocity of the residual nucleus, combined with the known lifetimes of the level and the gas cell dimensions we have calculated that the two effects will cancel out to within 2%. Because of the relatively large amount of Doppler broadening resulting from the use of a gas target, it was in some cases necessary to use known branching ratios and nonground-state transitions to separate unresolved multiplets. The mean Doppler shifts of isolated lines from evaporation residues were found to be in good agreement

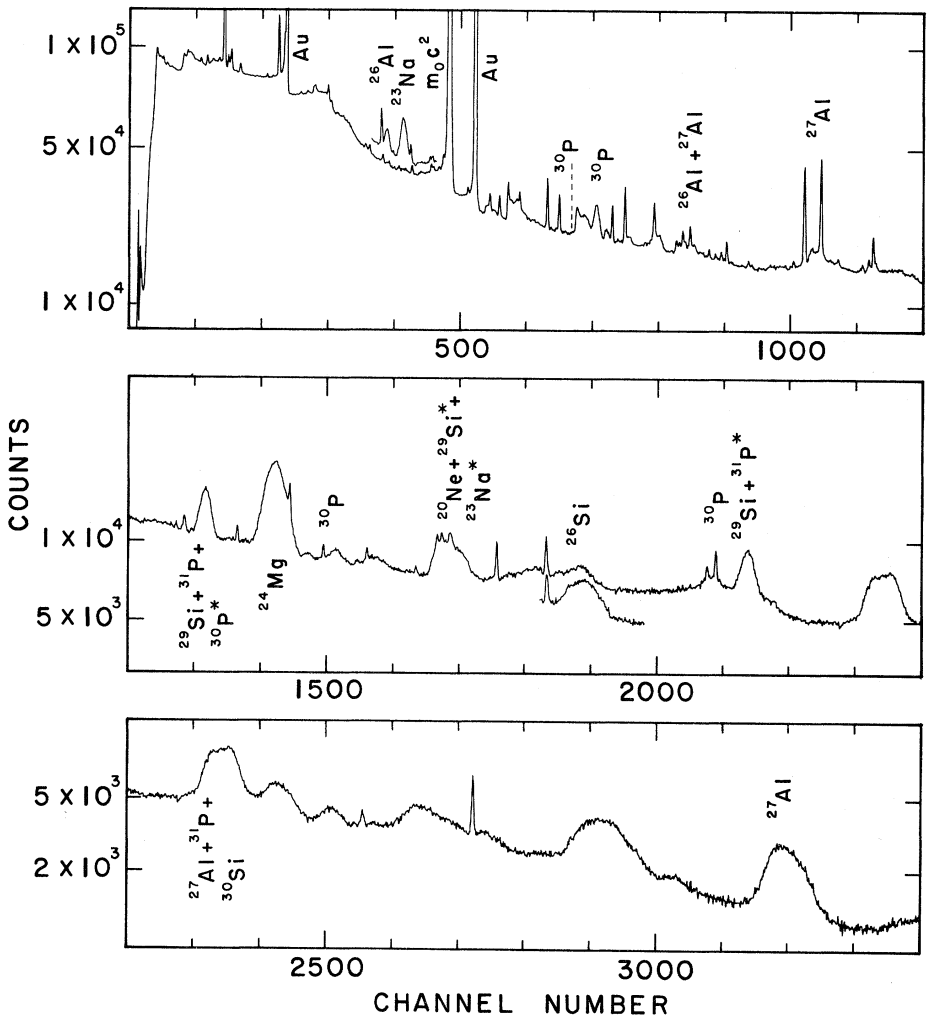

FIG. 2. A γ-ray spectrum from the $^{12}C+^{20}Ne$ reaction at $E_{c.m.}=21$ MeV. The insets near channels 400 and 1900 are from a spectrum taken at $E_{c.m.}=25$ MeV. The ground state transitions used to form the partial and total yields are labeled while nonground-state contaminants to these transitions are marked with an asterisk. The Au Coulex lines present are due to the Au beam stop.

with the calculated shifts assuming that evaporation residues have the same velocity as the initial compound system. Similarly, the mean Doppler shifts of observed multiplets resulting only from transitions in evaporation residues were found to be consistent with the calculated value. In contrast, the 1634-keV line in ^{20}Ne (which also includes components from transitions of a similar energy in ^{23}Na and ^{29}Si) displays a very small mean Doppler shift, corresponding to that expected if the ^{20}Ne component results from direct inelastic scattering at c.m. energies below $\sim$24 MeV. At higher energies, the measured mean Doppler shift of this line increases in a manner which suggests an increasing component of ^{20}Ne formed by 3α evaporation from the compound system. Note that there is some uncertainty with regard to the identification of the 1795 keV line (Table I) which we have ascribed to ^{26}Si on the basis of the energy of the line and the shape and strength of its associated excitation function. The unshifted energy for this transition was determined by measuring the observed Doppler shift as a function of angle and obtaining the intercept from a least-squares fit, which yielded a value of 1795.07 ± 0.57 keV after correction for the second-order Doppler effect. This is in good agree-

TABLE I. Gamma-ray transitions observed from the $^{12}C+^{20}Ne$ reaction.

Nuclide	Evaporated particles	E_γ (keV)
^{20}Ne	3α[a]	1633.7
^{23}Na	$2\alpha p$	439.9
^{24}Mg	2α	1368.6
^{26}Al	αnp	416.9, 829.6[b,c]
^{26}Si	$\alpha 2p$	1795.9
^{27}Al	αp	843.8,[c] 1014.5, 2210.5,[c] 2299.7,[d] 3004.2
^{29}Si	$2pn$	754.9,[d] 1273.3,[c] 1595.3,[d] 2028.2,[c]
^{30}P	pn	677.2, 709.0, 1264.0,[c,d] 1454.0, 1973.0, 2537.9
^{30}Si	$2p$	2235.4[c]
^{31}P	p	1266.1,[c] 2233.7,[c] 2028.8[c,d]

[a]This residual nuclide also results from direct reactions (see text).
[b]$1^+ \rightarrow 0^+$ transition to the 228 keV isomeric state.
[c]Member of an unresolved multiplet.
[d]Nonground-state transition not included in the total fusion yield.

ment with the tabulated[13] energy of 1795.90 ± 0.20 keV for the $2^+ - 0^+$ transition in ^{26}Si. However, we have been unable to observe the γ rays which should result from β^+ decay of ^{26}Si to the first excited state of ^{26}Al.

Excitation functions for the production of several of the observed nuclides are shown in Figs. 3–12. These include ^{24}Mg, ^{23}Na, ^{20}Ne, ^{26}Si, ^{30}P, ^{27}Al, ^{29}Si ($+^{31}P$), $^{30}Si+^{31}P$, and the total fusion yield. Also shown (Fig. 11) is the excitation function of the complex multiplet at $E_\gamma = 1267$ keV, which contains additional components of the ^{29}Si and ^{31}P reaction yields, as well as a nonground-state transition in ^{30}P. In each case, the error bars indicated are statistical uncertainties in the peak intensities, added in quadrature to the 1.5% rms deviation in the relative normalization discussed above. On the basis of a statistical analysis of repeated observations (90 individual measurements at 43 different energies), it appears that these errors slightly overestimate the true uncertainty. Possible systematic uncertainties include summing effects, which have been found to be negligibly small in the experimental geometry used, and γ-ray angular distribution effects. In previous experiments,[1,2,12] angle-integrated γ-ray yields were obtained from measurements of the excitation function at angles of 90° and 55° to the beam. However, it was found that the effect of P_4 and higher terms in the angular distribution made only a few-percent correction to the yield measured at 55°, and that this correction changed very slowly and smoothly with beam energy. In the present experiment, therefore, data were only taken at 55°.

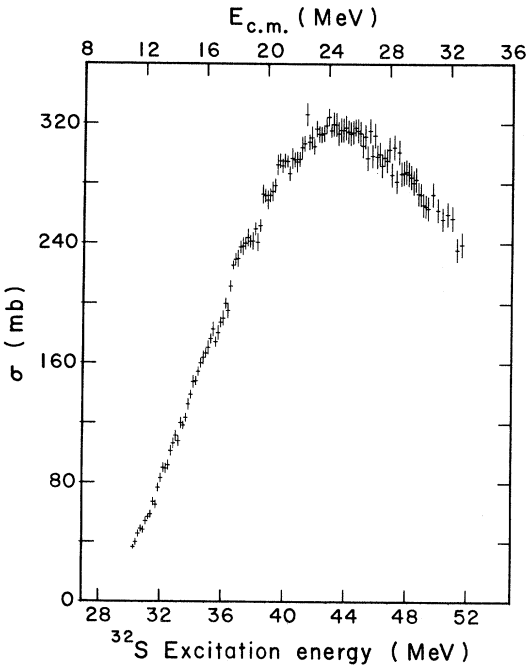

FIG. 3. The excitation function for the production of ^{24}Mg measured in the present experiment.

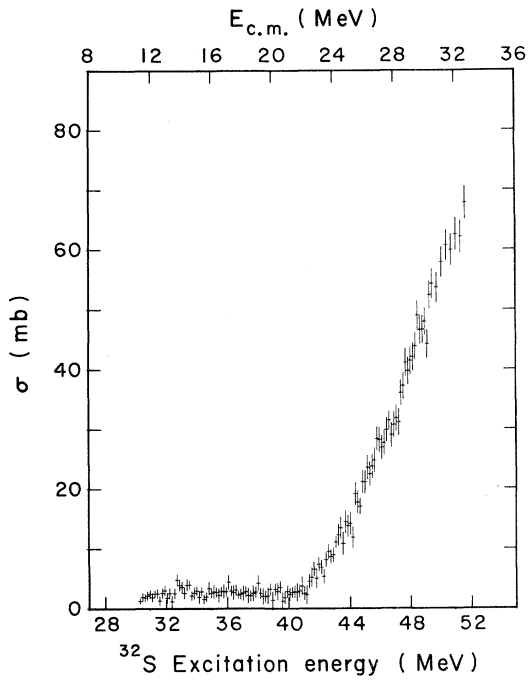

FIG. 4. The excitation function for the production of ^{23}Na measured in the present experiment.

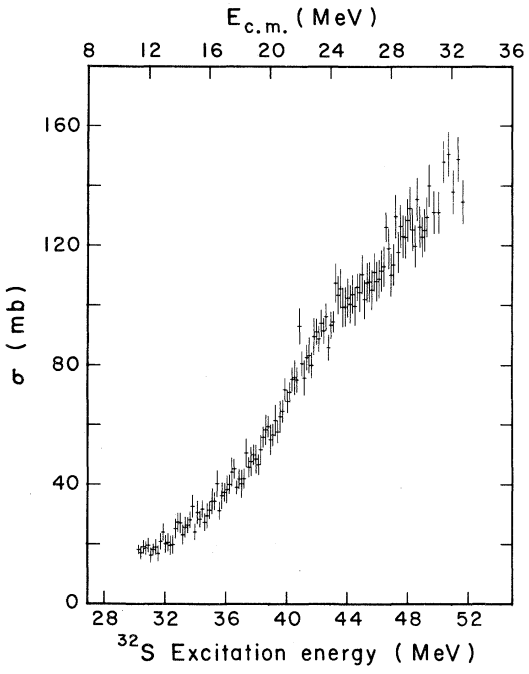

FIG. 6. The excitation function for the production of ^{26}Si measured in the present experiment.

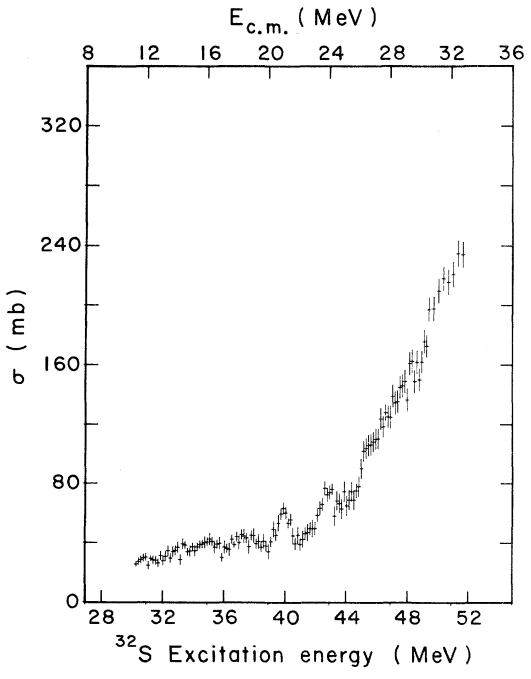

FIG. 5. The excitation function for the production of ^{20}Ne measured in the present experiment.

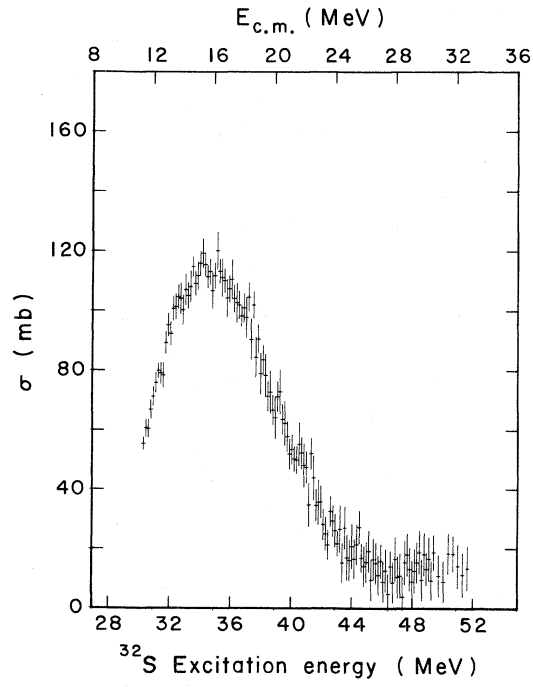

FIG. 7. The excitation function for the production of ^{30}P measured in the present experiment.

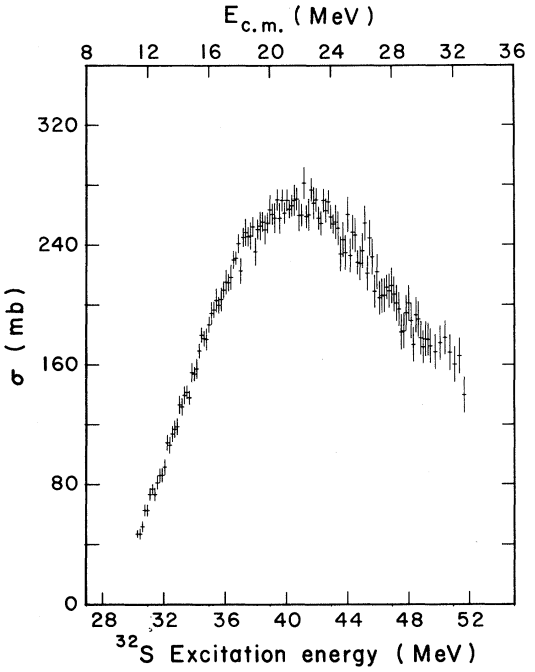

FIG. 8. The excitation function for the production of ^{27}Al, excluding decays through the 829.6 keV transition, measured in the present experiment.

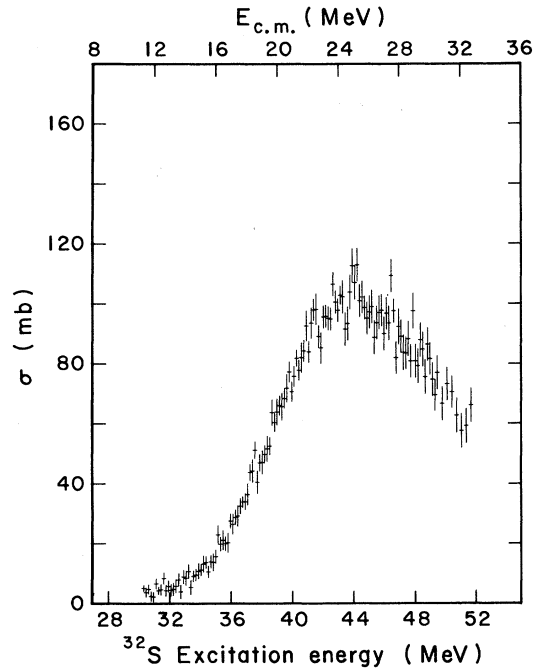

FIG. 9. The excitation function for the production of the $^{29}Si+^{31}P$ doublet at 2028 keV measured in the present experiment. Note that the ^{31}P contribution to this doublet results from a nonground-state transition and is not included in the total fusion yield.

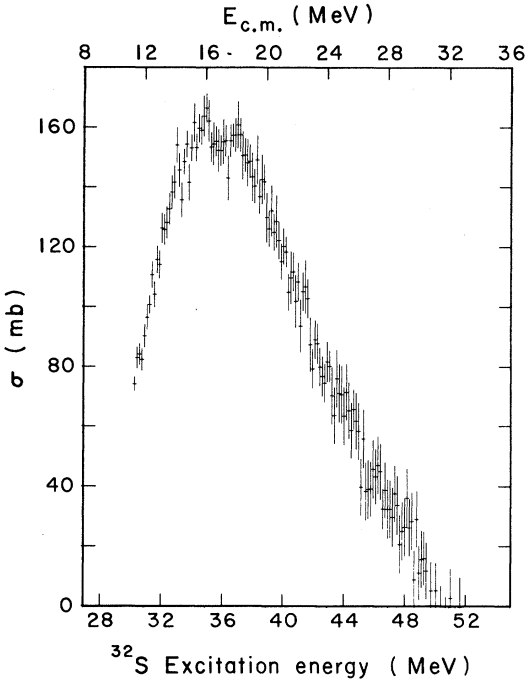

FIG. 10. The excitation function for the production of $^{30}Si+^{31}P$ (2234 and 2235 keV) measured in the present experiment. Note that the 1266 keV ground state transition in ^{31}P has been included in the complex multiplet shown in Fig. 11 rather than here.

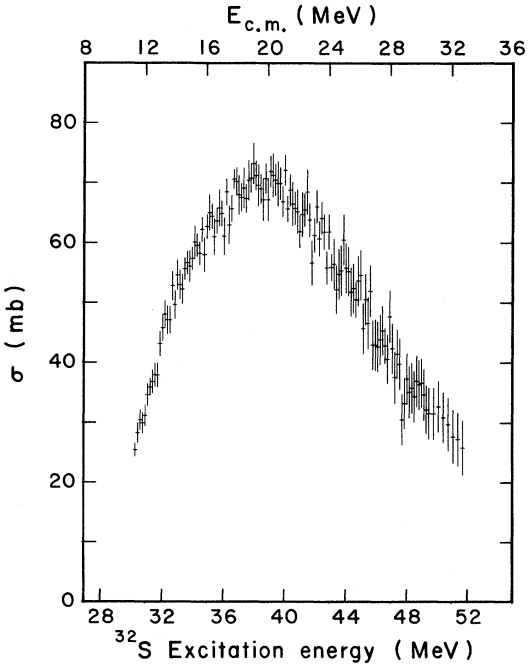

FIG. 11. The excitation function for the complex multiplet at $E_\gamma=1267$ keV, which contains ^{29}Si and ^{31}P ground state transitions as well as a nonground-state transition (not included in the total yield) in ^{30}P.

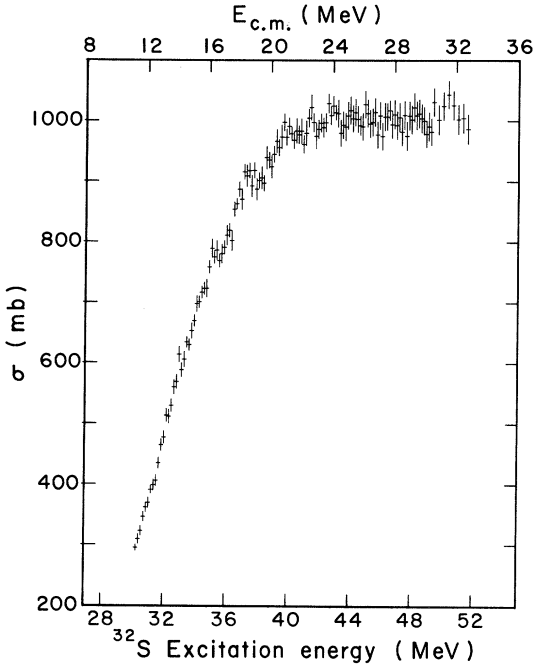

FIG. 12. The excitation function for the total fusion cross section measured in the present experiment.

III. DISCUSSION

A. Comparison with the $^{16}O+^{16}O$ production cross sections

Partially smoothed excitation functions for the observed exit channels from the $^{12}C+^{20}Ne$ and $^{16}O+^{16}O$ systems are compared in Fig. 13 as a function of excitation energy in the ^{32}S compound system. It can be seen that most channels display similar behavior in the two cases. The differences which are evident in the low-energy portion of the ^{20}Ne excitation function can be understood as being due to a strong component of direct inelastic scattering in the $^{12}C+^{20}Ne$ system, leaving the ^{20}Ne target in its first excited state. The corresponding direct α-transfer process in the $^{16}O+^{16}O$ system is much weaker, as expected. At the higher energies, 3α evaporation begins to be important and the similarity to the $^{16}O+^{16}O$ system is restored. There is also a tendency (visible in the yields of ^{23}Na, $^{26,27}Al$, and $^{30}Si+^{31}P$) for evaporation channels involving the emission of an α particle to be stronger in the case of $^{16}O+^{16}O$, while light-particle evaporation is somewhat favored in the $^{12}C+^{20}Ne$ reaction. This

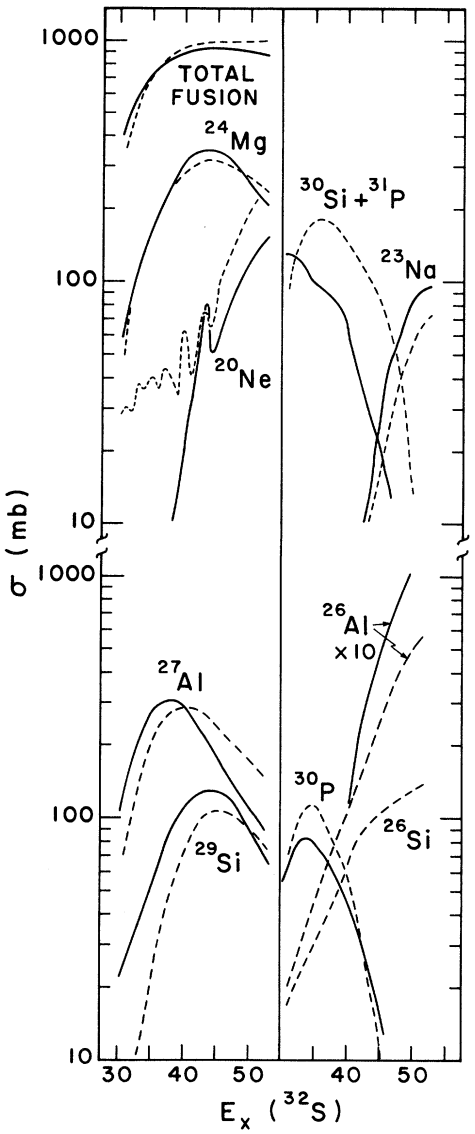

FIG. 13. Partially smoothed excitation functions from the $^{12}C+^{20}Ne$ system (dashed curve) and from the $^{16}O+^{16}O$ system (Ref. 2, solid curve) compared as a function of the excitation energy of the compound system.

behavior can be qualitatively understood in terms of the fact that the angular momentum brought in by the ^{12}C projectile is slightly less than that for ^{16}O at the same excitation energy in ^{32}S. However, the magnitude of the effect on the $^{30}Si+^{31}P$ excitation functions is surprisingly large, and the contrary behavior of the ^{29}Si yield is not explained. Finally, we note the anomalous behavior of ^{26}Si in the two systems, viz., the fact that it is strongly produced in

the $^{12}C+^{20}Ne$ reaction but apparently not at all in $^{16}O+^{16}O$.

It is instructive to compare the gross structure observed in the two systems. First of all, it is clear that regular oscillations are observed in the $^{12}C+^{20}Ne$ total fusion cross section (Fig. 12) just as for $^{16}O+^{16}O$. While the peak-to-valley ratio of the oscillations is not quite as large for $^{12}C+^{20}Ne$, it is difficult to understand why such structure should be observed at all. Not only are the $^{12}C+^{20}Ne$ optical-model potentials, such as that of Vandenbosch *et al.*,[9] far too absorptive to predict such oscillations, but it also appears that in the absence of identical-particle effects even the $^{16}O+^{16}O$ reaction cross section is predicted to be smooth. That is, the structure in the fusion cross section for $^{16}O+^{16}O$ results from the fact that odd-l partial waves are forbidden by symmetry, while a given partial wave is active over only a limited range of c.m. energies. The persistence of this feature of the $^{16}O+^{16}O$ fusion cross section to asymmetric systems such as $^{12}C+^{20}Ne$, where all partial waves are expected to contribute, is unexpected and has no immediately obvious explanation.

The intermediate-width structure observed primarily in the ^{20}Ne exit channels from the two systems is also of interest. We have already noted that the production of ^{20}Ne from the $^{12}C+^{20}Ne$ system below $E_x(^{32}S)=41.0$ MeV is predominantly due to direct inelastic scattering. It can be seen that there are several resonantlike anomalies in this energy range (Fig. 5). The most prominent of these is the one at $E_x=40.0$ MeV which has previously been observed by Ford *et al.*[14] in back-angle inelastic-scattering studies. This particular resonance is not correlated in any other exit channel, nor is it observed in the $^{16}O+^{16}O$ system, suggesting a possible odd-parity assignment. On the other hand, the strong anomaly at $E_x=43.0$ MeV is correlated in several reaction channels and has been observed in the work of Ford *et al.* and also in the $^{16}O+^{16}O$ system. The characteristic shape of the anomaly (slowly rising on the low energy side, followed by a rapid drop on the high-energy side) is also apparent in the corresponding $^{16}O+^{16}O$ resonance. This structure will be discussed in more detail below. Finally, we note that there are indications in Fig. 5 of a sequence of broader and weaker structures below $E_x=40$ MeV, some of which appear to be correlated in several reaction channels. Although these anomalies are poorly defined in the present data set, it would certainly appear to be interesting to investigate the $^{12}C+^{20}Ne$ inelastic scattering cross section in this low-energy region in more detail. The apparent anomaly at $E_x=45.2$ MeV, which may or may not be the same as the resonance reported in this energy region in Ref. 14, also deserves further study.

B. Comparison with other experiments

Four previous measurements of the $^{12}C+^{20}Ne$ fusion cross section are compared with the results of this work in Table II. Saint-Laurent *et al.*,[15] used heavy-particle detection techniques to determine σ_f at five isolated energies between $E_{c.m.}=25$ and 60 MeV. The total fusion cross sections reported in Ref. 15 are approximately 5% higher than those measured in the present work, but this is well within the mutual error of the two experiments.

TABLE II. Comparison of some measured fusion cross sections for $^{12}C+^{20}Ne$.

$E_{c.m.}$ (MeV)	σ (mb) present work	σ (mb) other	Ref.
12.13[a]	370±41	221±29[c]	18
15.0[a]	660±73	337±44[c]	18
25.2	1008±111	1070±95	15
26.0[b]	1020±112	931±93	16
30.0[b]	1050±111	1122±112	16
30.4	1010±111	1080±95	15
32.0[b]	1000±111	991±99	16
35.0[b]	1015±112	1041±104	16
41.25		1270±150	17

[a]Representative energies from the excitation function of Ref. 18.
[b]Representative energies from the excitation function of Ref. 16.
[c]Measured cross section (not "adopted" value). See text for discussion.

The partial elemental yields are found to be only in fair agreement, primarily due to a sizable disagreement as to the measured Al production at the higher energies. Possible reasons for this discrepancy include the difficulty in separating low velocity ions differing by only one unit of charge in heavy particle detection experiments, difficulty in separating Doppler-broadened multiplets in the γ-ray work, and the inability of γ-ray techniques to measure direct ground-state yields.

Tserruya *et al.*[16] also used heavy particle detection techniques to determine σ_f, in the energy range of $E_{\text{c.m.}}=24-42$ MeV. While the magnitude of σ_f reported in Ref. 16 is in reasonable agreement with the present data (Table I), the excitation function exhibits substantially different behavior from that observed in this work. In addition to the ambiguities discussed above in regard to the work of Saint-Laurent, another possible cause of this disagreement may be the fact that Tserruya *et al.* used natural, rather than isotopic, Ne as their target. The resulting 10% contamination of ^{22}Ne could easily result in the observed differences in the excitation function. An additional measurement at $E_{\text{c.m.}}=41.25$ MeV was made by Menet *et al.*,[17] who used particle detection combined with time-of-flight measurements to deduce partial and total yields. Their value for σ_f (1270 ± 150 mb) is somewhat larger than that measured by Tserruya *et al.* at the same energy.

The most recent measurement on the ^{12}C+^{20}Ne system is that reported by Hulke *et al.*,[18] who used γ-ray techniques and a differentially-pumped gas target. They determine the yield of a reaction product on the basis of measurements on one or two transitions from low-lying excited states. These measured cross sections are then corrected for missing yield by using known branching ratios and assuming a $2J+1$ population of high-lying levels, and the ground state, to arrive at an "adopted" yield. There are rather substantial disagreements between this work and the present experiment, the most serious of which occurs for the production of ^{27}Al (Table III) which is more than on order of magnitude larger in our work. In this case, we find that the majority of the ^{27}Al yield results in the occurence of 2210- and 3004-keV transitions. The latter of these is beyond the dynamic range of Ref. 18, while the former is included in a very complicated multiplet of lines near 2200 keV. The ^{27}Al contribution to this multiplet is estimated on the basis of known branching ratios[13] for the states at 3004 and 4510 keV. (The decay of the latter state results in a 2300-keV transition which is clearly separated in our spectra.) It appears that the correction factor applied to the measured yield in Ref. 18 does not completely compensate for the fact that the decays of these high-spin states were not directly observed. One other possible reason for disagreement between the two experiments is the effect of the angular distribution of the γ radiation. As discussed above, the integrated cross section may be substantially *greater* than the yield measured at 90° if the alignment is reasonably strong for $E2$ transitions such as are involved in the decay of ^{24}Mg. Hulke *et al.* report isotropic angular distributions at sub-Coulomb energies. Due to the design of our gas cell, we have been unable to reliably measure angular distributions since the solid angle subtended by the detector and the target thickness vary with angle. However, it has been found[2] for ^{16}O+^{16}O that the alignment is reasonably strong even at $E_{\text{c.m.}}=15$ MeV. It is particularly interesting in this regard to note that the total yield of ^{20}Ne, corrected for the angular distribution appropriate to Coulomb excitation,[18] is in good agreement in the two experiments over their region of overlap.

TABLE III. Comparison of measured yields from ^{12}C+^{20}Ne at $E_{\text{c.m.}}=14.95$ MeV.

Nuclide	σ (mb)[a] Ref. 15	σ (mb) Present work
^{31}P+^{30}Si	168 (205)	170
^{30}P	70 (110)	110
^{28}Si	11 (15)	
^{27}Al	13 (50)	160
^{24}Mg	76 (95)	140
Total fusion	337 (475)	660

[a]Values in parentheses are the "adopted" yields of Ref. 18.

C. Trajectory of the critical angular momentum

The critical angular momentum for fusion of nonidentical particles is deduced from the total fusion cross section using the sharp-cutoff model expression:

$$\sigma_f = \pi \lambda\!\!\!^{-2} (l_c + 1)^2 , \quad (1)$$

where $\lambda\!\!\!^{-}$ is the reduced wavelength. The experimental values of l_c for the $^{12}C+^{20}Ne$ fusion reaction deduced from the present work are shown in Fig. 14, where we plot excitation energy in the compound system versus $l_c(l_c+1)$ to bring out the quasirotational nature of the data. Also shown is the trajectory of the critical angular momentum for the total reaction cross section computed from the potential of Vandenbosch *et al.*[9] At first glance, the experimental trajectory of l_c in Fig. 14 appears to be relatively featureless, especially when compared with the situation for $^{16}O+^{16}O$. Nevertheless, many remarkable similarities can be seen upon closer examination and comparison with the results presented in Ref. 8 for fusion of $^{16}O+^{16}O$ and $^{12}C+^{16}O$. The first and most striking of these is the fact that a distinct change in the slope of the experimental trajectory occurs just as it intersects the straight line (Fig. 14) having moment-of-inertia parameter $\hbar^2/2\theta = 165$ keV which passes through the origin of the plot (the ground state of ^{32}S). We note that this same straight line also gives the best least-squares fit to the average high-energy behavior of the trajectory of l_c for $^{16}O+^{16}O$. In the present case, the critical angular momentum does not follow this straight line beyond the crossover point as for $^{16}O+^{16}O$. However, similar behavior to that seen here has been observed[8] for the nonidentical-particle $^{12}C+^{16}O$ reaction, and attributed to the fact that both even and odd spin states can be populated in these systems.

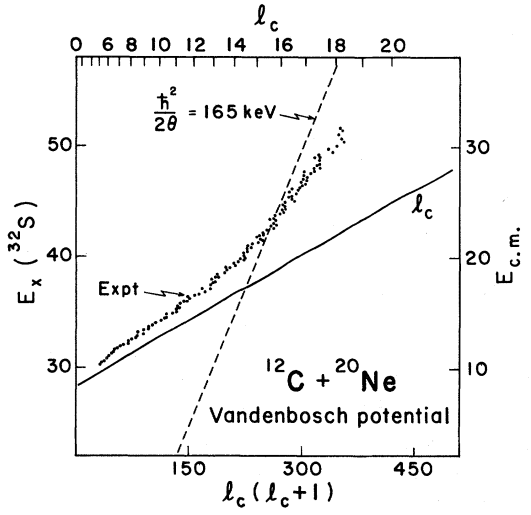

FIG. 14. The critical angular momentum trajectory for $^{12}C+^{20}Ne$ deduced from the measured total fusion cross section. The solid line is the critical angular momentum trajectory deduced from the reaction cross section calculated with the potential of Ref. 9. The trajectory for the grazing angular momentum is almost identical to that of the critical angular momentum.

The second remarkable feature of the $^{12}C+^{20}Ne$ cross sections is the fact that the crossing point, at $E_x(^{32}S)=43.0$ MeV, is correlated with a strong resonancelike structure which appears in several reaction channels but is most apparent in the yield of ^{20}Ne (Figs. 5 and 13), as was already mentioned above. This is, in fact, the characteristic resonance which has been shown to be associated with the transition to the limited-fusion regime in several light heavy-ion systems. It is visible in the critical-angular-momentum plot (Fig. 14) as the nearly vertical segment at $E_x=43.0$ MeV and $l_c=16$. We note that this is exactly the excitation energy and critical angular momentum found for the $^{16}O+^{16}O$ characteristic resonance.[8]

Less obvious in Fig. 14, but readily apparent in the reaction cross sections, are anomalies at $E_x=41.6$, 37.5, 35.5, and possibly 32.5 MeV, with associated l_c values of 15, 13, 11, and 9, respectively. The first of these is particularly interesting since it corresponds to a prominent, narrow resonance which is correlated in several reaction channels. This is *not* the resonance of Ford *et al.*,[14] which occurs at $E_x=40.0$ MeV and is visible in Fig. 12 as a small anomaly at that energy. It would be very desirable to have a spin/parity assignment for the $E_x=41.6$ MeV resonance. However, the appropriate experiment is liable to be difficult since the resonance is not observed in the ^{20}Ne channel. If we accept the association of this structure with $l_c=15$, and of the lower-energy anomalies with consecutive odd l values as suggested from the trajectory in Fig. 14, then a pattern emerges in which the odd-l partial waves are enhanced over the even-l partial waves in this range of c.m. energies. That is, the nuclear surface appears to be more transparent to odd-l than even-l partial waves prior to reaching the limited-fusion regime. This behavior suggests the use of an optical-model potential which contains an explicit parity-dependent absorption. Parity dependent optical-model potentials have been exam-

ined by Chan *et al.*[19] in an effort to reproduce the structure observed in the fusion yields from the $^{12}C+^{16}O$ system. The method chosen to effect the parity dependence was to scale the entire real and/or imaginary well by a factor $1+b(-1)^l$. They report very little success with this approach and concluded that parity dependent effects were unlikely to be the cause of the observed structure. In light of this work, and noting that the "extreme" surface transparent potential of Gobbi *et al.*[20] approximately reproduces the magnitude and periodicity of structure in the $^{16}O+^{16}O$ reaction cross section, we attempted calculations in which only a surface-peaked term of the imaginary potential was varied according to the parity of the incoming partial wave. Specifically a term of the form

$$A_p(-1)^l\frac{1}{r}\left|\frac{d}{dr}V_{\rm re}(r)\right|, \tag{2}$$

where A_p is the magnitude of the parity dependence, l is the particular incoming partial wave, and $V_{\rm re}$ is the real potential, was added to the imaginary well of the potential given in Ref. 9. Care was taken to insure that a particular value of A_p did not result in an unphysical imaginary well, i.e., one which was positive, or a great deal more negative than the depth of the well at the origin, in the region of the nuclear surface. To date, all calculations using this parity-dependent term have been unsuccessful in reproducing the observed behavior of the $^{12}C+^{20}Ne$ system. We conclude that the potential of Ref. 9 is far too absorptive for the parity-dependent term to have the desired effect.

V. CONCLUSION

Excitation functions for the production of ten nuclides in the $^{12}C+^{20}Ne$ reaction have been measured over the energy range $E_{\rm c.m.}=11-33$ MeV. Comparison with previous data for the $^{16}O+^{16}O$ system shows that the long-term behavior of most reaction yields is similar in the two cases. Some of the remaining differences can be understood as due to strong components of direct inelastic scattering in the $^{12}C+^{20}Ne$ system. This close similarity is expected on the basis of the fact that $^{12}C+^{20}Ne$ and $^{16}O+^{16}O$ are well-matched systems in the sense that, at a given excitation energy in the ^{32}S compound nucleus, the angular momenta brought in by the two reactions are nearly the same.

On a less global scale, we observe that regular structure occurs in the individual nuclide yields, and also in the $^{12}C+^{20}Ne$ total fusion cross section. The persistence of these oscillations, which are a characteristic feature of the $^{16}O+^{16}O$ reaction cross sections, to such asymmetric systems as $^{12}C+^{20}Ne$ is unexpected. It appears that the explanation of this phenomenon must involve some mechanism to enhance the structure due to certain partial waves over that predicted by the optical model. The regular nature of these oscillations suggests parity dependence in the optical-model potential. However, attempts to produce such structure by adding a parity-dependent term to a $^{12}C+^{20}Ne$ optical-model potential taken from the literature[9] have been unsuccessful. Further studies might involve additional elastic and inelastic scattering measurements in an attempt to determine whether less-absorptive optical-model potentials might be able to fit both the elastic scattering and reaction data.

A most prominent resonance, at $E_{\rm c.m.}=21.1$ MeV in the $^{20}Ne(2^+)$ inelastic scattering yield, appears not to be correlated in any other exit channels from the $^{12}C+^{20}Ne$ system. This anomaly has previously been seen[14] in the work of Ford *et al.* Another resonance, at $E_{\rm c.m.}=22.7$ MeV, is particularly interesting because of its rather small width and the fact that it is correlated in several reaction channels. It would be very interesting to have a spin/parity assignment to this structure, but the appropriate experiment is liable to be difficult since the resonance does not appear in the inelastic-scattering excitation function. Finally, a structure at $E_{\rm c.m.}=24.1$ MeV in this same ^{20}Ne excitation function is correlated in several other reaction channels and furthermore has the same characteristics as a resonance previously observed in the $^{16}O+^{16}O$ reaction at the same excitation energy in the ^{32}S compound system.

In conclusion, we have observed several new features of the $^{12}C+^{20}Ne$ reaction cross sections. The most remarkable of these are the fact that regular oscillatory structure occurs in this system as well as in the $^{16}O+^{16}O$ reaction, and the observation that a "characteristic" resonance, which appears at $E_x(^{32}S)=43.0$ MeV and $l_c=16$, has the same properties as a similar structure observed at the identical excitation energy in the $^{16}O+^{16}O$ reaction yields. This result lends further weight to the empirical observation that these characteristic resonances, which are found to be associated with the transition to the regime of limited fusion, are a property of the compound system rather than of the entrance channel.

This work was supported by the National Science Foundation, under Grant No. PHY 80-08234.

[1]J. J. Kolata, R. M. Freeman, F. Haas, B. Heusch, and A. Gallmann, Phys. Rev. C 16, 891 (1977).
[2]J. J. Kolata, R. M. Freeman, F. Haas, B. Heusch, and A. Gallmann, Phys. Rev. C 19, 2237 (1979).
[3]I. Tserruya, Y. Eisen, D. Pelte, A. Gavron, H. Oeschler, D. Berndt, and H. L. Harney, Phys. Rev. C 18, 1688 (1978).
[4]B. Fernandez, C. Gaarde, J. S. Larsen, S. Pontoppidan, and F. Videbaek, Nucl. Phys. A306, 259 (1978).
[5]V. K. C. Cheng, A. Little, H. C. Yuen, S. M. Lazarus, and S. S. Hanna, Nucl. Phys. A322, 168 (1979).
[6]D. G. Kovar, D. F. Geesaman, T. H. Braid, Y. Eisen, W. Henning, T. R. Ophel, M. Paul, K. E. Rehm, S. J. Sanders, P. Sperr, J. P. Schiffer, S. L. Tabor, S. Vigdor, B. Zeidman, and F. W. Prosser, Jr., Phys. Rev. C 20, 1305 (1979).
[7]J. V. Maher, M. W. Sachs, R. H. Siemssen, A. Weidinger, and D. A. Bromley, Phys. Rev. 188, 1665 (1969).
[8]J. J. Kolata, Phys. Lett. 95B, 215 (1980).
[9]R. Vandenbosch, M. P. Webb, and M. S. Zisman, Phys. Rev. Lett. 33, 842 (1974).
[10]P. A. DeYoung, J. J. Kolata, R. C. Luhn, R. E. Malmin, and S. N. Tripathi, Phys. Rev. C 24, 166 (1981).
[11]Program SWHET obtained from Dr. R. O. Sayer, Oak Ridge National Laboratory (unpublished).
[12]J. J. Kolata, R. M. Freeman, F. Haas, B. Heusch, and A. Gallman, Phys. Rev. C 19, 408 (1979).
[13]R. J. de Meijer, A. G. Drentje, and H. S. Plendl, At. Data Nucl. Data Tables 15, 391 (1974).
[14]J. L. C. Ford, Jr., J. Gomez del Campo, D. Shapira, M. R. Clover, R. M. DeVries, B. R. Fulton, R. Ost, and C. F. Maguire, Phys. Lett. 89B, 48 (1979).
[15]F. Saint-Laurent, M. Conjeaud, and S. Harar, Nucl. Phys. A327, 517 (1979).
[16]I. Tserruya, J. Barrette, S. Kubono, P. Braun-Munzinger, M. Gai, and C. D. Uhlhorn, Phys. Rev. C 21, 1864 (1980).
[17]J. Menet, A. J. Cole, N. Longequeue, J. J. Lucas, G. Mariolopoulos, J. B. Viano, J. C. Saulnier, and D. H. Koang, J. Phys. 38, 1051 (1977).
[18]G. Hulke, C. Rolfs, and H. P. Trautvetter, Z. Phys. A 297, 161 (1980).
[19]Y. D. Chan, H. Bohn, R. Vandenbosch, K. G. Bernhardt, J. G. Cramer, R. Sielemann, and L. Green, Nucl. Phys. A303, 500 (1978).
[20]A. Gobbi, R. Wieland, L. Chua, D. Shapira, and D. A. Bromley, Phys. Rev. C 7, 30 (1973).